

T. Lang, M. A. Odnoblyudov, V. E. Bougrov, M. Sopanen, MOCVD growth of GaN islands by multistep nucleation layer technique, *Journal of Crystal Growth* 277 (2005) 64.

© 2005 Elsevier Science

Reprinted with permission from Elsevier.



MOCVD growth of GaN islands by multistep nucleation layer technique

T. Lang^{a,*}, M. Odnoblyudov^b, V. Bougrov^b, M. Sopanen^a

^a*Electronics and Telecommunications Optoelectronics Laboratory, Helsinki University of Technology, P.O. Box 3500, FIN-02150 HUT, Espoo, Finland*

^b*Abraham Ioffe Physico-Technical Institute, Politekhnicheskaya 26, 194021 St.Petersburg, Russian Federation*

Received 14 October 2004; accepted 5 January 2005

Communicated by R.M. Biefeld

Available online 11 February 2005

Abstract

The widely adopted two-step growth process can reduce problems caused by lattice mismatch in growing gallium nitride (GaN) with metal-organic chemical vapor deposition on a sapphire substrate. The method involves a low-temperature GaN deposition step followed by a high-temperature one in which GaN island coalescence is followed by a quasi-two-dimensional growth mode. In this paper, a multistep growth method for controlling the size of hexagonal GaN islands on sapphire substrates is introduced. The method involves alternate low-temperature growth and recrystallization steps to increase the size of GaN clusters in a controlled manner. Hexagonal GaN islands with good crystalline quality are grown by metal-organic chemical vapor deposition in a vertical-flow close-coupled showerhead reactor. Reflectometry is used to monitor film growth in situ. The morphology of the resulting GaN films is determined using atomic force microscopy. Also, the crystalline structure and quality of the GaN islands are assessed by X-ray diffraction and transmission electron microscopy. Results clearly indicate gradual increase in island size after each recrystallization step without any observable change in island density relative to the first recrystallization step. Merging of GaN islands is evident after four cycles of the multistep growth process.

© 2005 Elsevier B.V. All rights reserved.

PACS: 81.15.Gh; 68.55.-a

Keywords: A1. Atomic force microscopy; A1. Nucleation; A1. Recrystallization; A3. Metalorganic chemical vapor deposition; B1. GaN

1. Introduction

The wide variety of potential applications of III–V nitride semiconductors has drastically increased the research activity related to these

*Corresponding author. Tel.: +358 40 576 3796; fax: +358 9 451 3128.

E-mail address: teemu.lang@hut.fi (T. Lang).

materials. Especially, the demonstration of bright blue light emitting diodes (LEDs) and blue laser diodes (LDs) [1–3] has proven nitride-based semiconductors to be a promising material system for high-power and high-speed optoelectronic devices.

One of the main difficulties in the crystal growth of high-quality gallium nitride (GaN)-based devices is the lack of lattice-matched substrates. Lattice mismatch leads to high threading dislocation (TD) densities in nitride films. Although blue-light emission was observed in films where the TD density is on the order of $5 \times 10^{10} \text{ cm}^{-2}$ [4] TDs were been shown to have detrimental effects on radioactive carrier recombination and carrier transport [5,6]. In order to improve the crystalline quality of heteroepitaxial GaN layers grown by metal-organic chemical vapor deposition (MOCVD) on hexagonal Al_2O_3 (sapphire) substrates, a two-step growth process has been adopted [7]. This method involves deposition of a thin nucleation layer (NL) at a lower temperature (LT) followed by a high-temperature (HT) growth phase. Upon temperature ramping from LT to HT the NL is annealed. LT-GaN nucleation layers were shown to grow predominantly in the cubic (111) phase on a sapphire (0001) “*c*-plane” surface [8–10]. The temperature ramping recrystallizes the film to increase the hexagonal (0001) content, while roughening the morphology of the film into more island-like character [8,9]. It was previously shown that the LT NL growth conditions and the resulting microstructure and surface morphology after recrystallization are critical for the quality of HT-GaN films [9]. In order to optimize the growth conditions and the starting surface for the subsequent HT-GaN growth it would be beneficial to be able to efficiently control the size and shape of the islands acting as nucleation centers.

Significant amount of work has been carried out with the goal of reducing TD density in HT-GaN by optimizing the growth conditions of the LT-GaN film and thereby the surface morphology and crystalline quality of recrystallized NLs [9,11–13]. Also, Iwaya et al. [14] have studied the effect of multiple buffer layers on the quality of HT-GaN on sapphire. They showed that the etch pit density

(EPD) reduces drastically upon insertion of an additional LT-AlN or LT-GaN nucleation layer into the HT-GaN layer. The same paper also reports an increase in EPD when two nucleation layers were deposited consecutively on top of each other prior to the HT stage of the growth process. Both these NLs were 20 nm thick and were annealed individually to 1050 °C for recrystallization.

The purpose of this work is to study a new MOCVD growth method for controlling the surface morphology of an annealed LT-GaN nucleation layer. The possibility of accurately changing the size and shape of nucleation centers for a subsequent HT growth stage would be of help in optimizing the NL morphology. In this paper, we report that the size of GaN islands can be efficiently controlled independent of their density by the use of consecutive LT-GaN deposition and annealing steps. The method also gradually changes the shape of the nucleation centers as their cross-section parallel to the substrate become more hexagon shaped.

2. Experimental procedure

The studied GaN films were grown in a vertical flow 3×2 ” close-coupled showerhead MOCVD reactor. The precursors used for gallium and nitrogen were TMGa and NH_3 , respectively. Hydrogen was used as carrier gas throughout every growth run. The substrates were 2” *c*-plane epi-ready sapphire wafers. Before deposition, the substrates went through an in situ annealing at 1070 °C for 300 s in a hydrogen atmosphere. Subsequent surface nitridation was carried out at 530 °C with an ammonia flow of 89 mmol min^{-1} for 300 s.

An LT NL deposition and annealing cycle consisted of 115 s of GaN deposition at 530 °C followed by a 300 s temperature up-ramp (linear) to 1060 °C and an immediate 120 s down-ramp (linear) back to 530 °C. A growth rate of $1.04 \mu\text{m h}^{-1}$ and a V/III-ratio of 1500 were used during the LT deposition phase. The growth rate was calculated based on the reflectometer data obtained during a calibration run. In this run,

a thick layer of LT-GaN was grown in conditions identical to the LT films in the studied samples. During each step of the LT NL cycle, the ammonia flow and total pressure were kept at constant 89 mmol min^{-1} and 500 Torr, respectively. Three films were studied. They consisted of one (sample A), two (sample B) and four (sample C) deposition and annealing cycles. After the last annealing step each sample was cooled down to 470°C in an ammonia–hydrogen atmosphere and subsequently to room temperature (RT) in a hydrogen atmosphere.

The reflectance from growing films was monitored in situ with a reflectometer operating at a wavelength of 637.8 nm in a normal incidence mode. A laser beam with a spot size of approximately 2 mm in diameter on the sample surface was fed to the reactor through a quartz probe located on top of the showerhead. The reflected signal was detected with an Si-photodiode via a semitransparent mirror. The surface morphology of each sample was examined with a NanoScope IIE atomic force microscope (AFM). Crystalline quality was also evaluated by X-ray diffraction (XRD) and transmission electron microscopy (TEM). The XRD was a high-resolution Philips X'Pert system that was used in a triple-axis configuration where an analyzer crystal is placed in front of the detector to maximize angular resolution.

3. Results and discussion

In situ reflectometry data in Fig. 1 were recorded during the growth of sample C. The data for samples A and B are identical to sample C up to the point where each sample is cooled down. After this point, the reflectivity remains constant. In the figure, these points in time are labeled with arrows A, B and C for samples A, B and C, respectively. The reflectivity data clearly indicate four cycles during which LT-GaN deposition and annealing take place as described in Section 2. In the inset of Fig. 1, the critical points of the reflectivity transient of one cycle of LT deposition are labeled. The shape of this curve is typical for LT-GaN deposition followed by an annealing step

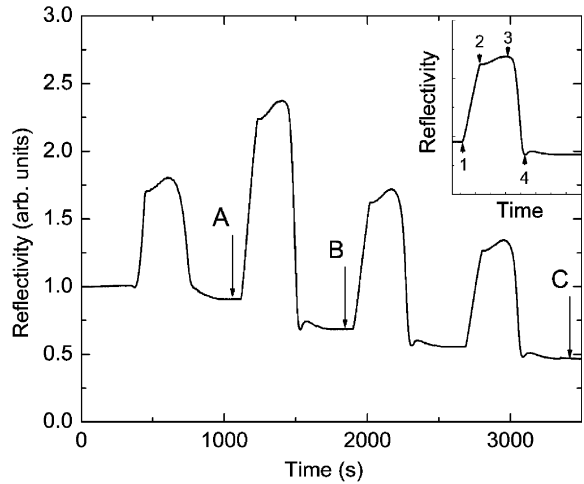


Fig. 1. In situ reflectometry data recorded during the growth of sample C. Points A, B and C designate the times at which the growth of each sample (A, B and C, respectively) was terminated. The critical points of one LT deposition and recrystallization cycle can be seen in the inset.

[8,15]. Film deposition occurs between points 1 and 2 as predominantly cubic (1 1 1) oriented GaN is grown [8–10]. During this time the reflectivity increases due to constructive interference between the wavefront reflected from the film surface and the wavefront reflected from the GaN-sapphire interface. After the interruption of film growth the slower increase in reflectivity starting from point 2 is caused by the increase in the refractive index of GaN as a function of temperature. This increase in reflectivity takes place during the beginning of the temperature up-ramping stage (between points 2 and 4) until point 3 is reached.

As temperature up-ramping is continued beyond point 3, island formation starts at approximately 900°C . This event is accompanied by surface roughening causing the reflectivity to decrease. There is evidence that the transformation in surface morphology is mediated by desorption, surface diffusion and redeposition processes during which hexagonal GaN is deposited on top of disordered phase material [8,10]. This material redistribution process involves a ripening phenomenon where smaller islands shrink and larger ones increase in size. The result is a bimodal distribution of GaN islands clearly visible in the AFM

data of Fig. 2. In this paper, terms such as “GaN island” and “GaN cluster” are used to address only the upper part, i.e. the larger islands of this bimodal size distribution unless otherwise stated. The exact mechanism governing the material redistribution process is not entirely clear at this point but it has been observed that GaN begins to decompose already at temperatures slightly above 800 °C in an H₂ ambient [16]. The decomposition reaction produces gaseous NH₃ and metallic Ga. Therefore, it can be argued that when GaN films are annealed in an ammonia-rich atmosphere, surface diffusivity of the Ga species [17] is the limiting factor of the material redistribution process. The ripening phenomenon and material transport during LT NL annealing are discussed in more detail in Ref. [8] and references therein.

Point 4 in the reflectivity transient of Fig. 1 signifies the time at which temperature down-ramping begins. From this point, reflectivity of the sample surface remains essentially unchanged before the next deposition cycle. After the last three temperature up-ramps, a slight increase in reflectivity in Fig. 1 is arguably caused by surface smoothening and refractive index changes as the slope of the temperature transient switches from positive to negative. If the temperature up-ramping was continued, the reflectivity would eventually reach the sapphire baseline value (scaled to unity in Fig. 1) as the recrystallized islands desorb revealing the bare sapphire surface.

As can be seen in Fig. 1, the minimum stabilized reflectivity during a temperature down-ramp gradually decreases after each cycle, reaching a minimum of about 0.5 at point C. This trend is due to increase in the size of GaN islands as depicted in the AFM micrographs of Fig. 2(a)–(c) which were obtained in deflection mode. These images, respectively, describe the surface morphology of samples A, B and C corresponding to points A, B and C in the reflectivity transient of Fig. 1. The AFM measurements suggest that the density of islands remains virtually unchanged at about $6 \times 10^7 \text{ cm}^{-2}$ after each cycle. Also, the background roughness in between the islands is similar for each sample. The average height of the islands in the samples A, B and C is 135, 375 and 410 nm, respectively, indicating that island growth in the [0001]

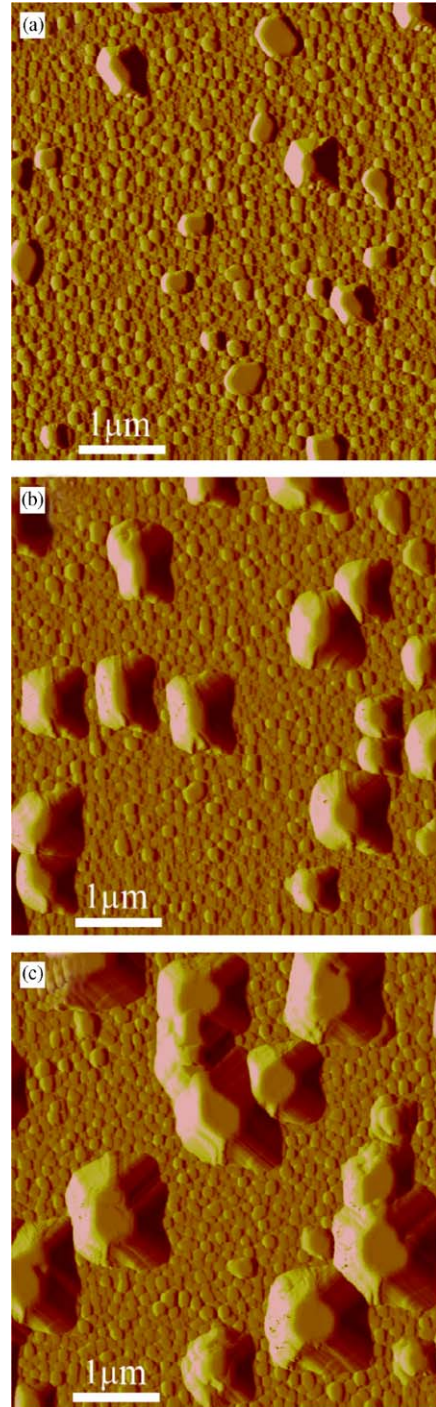


Fig. 2. Deflection mode AFM data depicting the surface morphology of (a) sample A, (b) sample B and (c) sample C. Vertical and horizontal scales are equal in each figure.

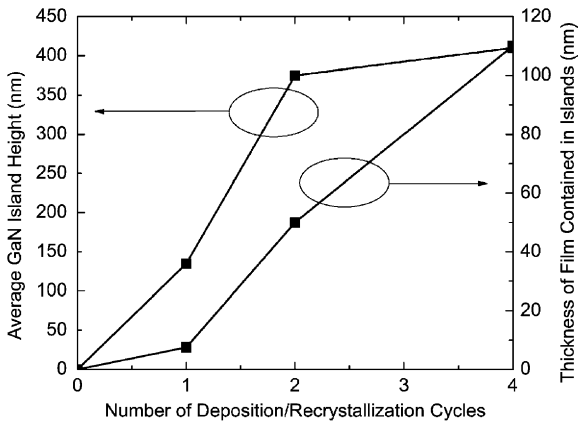


Fig. 3. Average GaN island height and thickness of the film contained in the islands after recrystallization as a function of the number of deposition cycles. Saturation of growth in the vertical direction can be observed after two cycles.

direction saturates after two cycles of LT GaN deposition (Fig. 3). The increasingly large flat area on top of most of the islands also suggests that the (0001) surfaces become stabilized after the growth has saturated in the [0001] direction. Similar results have been reported elsewhere [10].

Further calculations based on the measured AFM data show that nominally about 5–10 nm of film is contained in the GaN islands in the sample A. The corresponding nominal film thickness for islands in samples B and C are about 50 and 110 nm, respectively (Fig. 3). These results were obtained from the AFM height data with computer software by numerically calculating the volume of material that is contained in the nucleation islands and averaging this volume over the scanned $25\mu\text{m}^2$ area. The volume was also calculated by modeling the islands as cylinders having a diameter equal to the full-width at half of the maximum height of an island. The results from these two methods were the same within an error of a few nanometers of nominal film thickness. Since, based on the growth rate used, about 33 nm of LT-GaN is deposited in each cycle, we can conclude that during recrystallization virtually all of the deposited film nucleates on the existing islands were formed during the previous recrystallization phase.

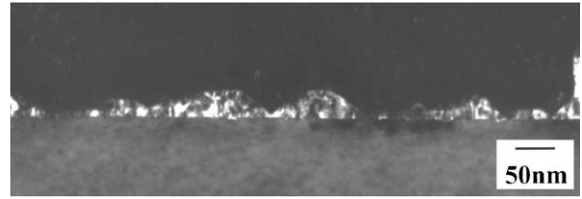


Fig. 4. A dark field cross-sectional TEM image bringing out the thickness variations in the thin deposit in between GaN nucleation islands. The data were obtained from sample C. Vertical and horizontal scales are equal in the figure.

The dark field cross-sectional TEM data of Fig. 4 show the cross-sectional profile of the deposit in between the GaN nucleation islands in sample C. Calculations based on the data give an average thickness of about 15–20 nm for this thinner deposit forming the background of the AFM images in Fig. 2. This result suggests that very little or none of the deposited LT material is lost by desorption during the recrystallization process. The measurements and calculations above support the observations by Lada et al. [8] who reported that only a minority (less than 10%) of the material is desorbed during an annealing stage similar to the one used in our study. Their results were obtained from cross-sectional TEM data, and modeling of in situ reflectivity transients supported the observations.

Due to the gradual increase in the island size, the starting surface for an LT deposition phase roughens after each annealing and recrystallization step. In the reflectivity data of Fig. 1, this can be seen as a decrease of slope in consecutive LT depositions. The effect should not be interpreted as a decrease in growth rate. This phenomenon is most likely caused by the fact that the constructive interference effect responsible for the increase in reflectivity is not as pronounced for a rougher film surface. The growth rate during the first LT deposition phase was also $1.04\mu\text{m h}^{-1}$ as determined from the calibration run and from the slope of the reflectivity transient. On the other hand, a reflectivity value of about 1.7 is reached during this first LT growth phase corresponding to a film thickness of only 21 nm. The discrepancy between this thickness value and the 33 nm film thickness expected for a 115 s growth period is attributed to

the initial GaN nucleation on sapphire surface. Careful analysis of the reflectivity data reveals an approximately 60 s delay before the first LT-GaN layer starts to grow at its normal rate after gas-phase decomposition of precursors has started. A study about the nucleation of GaN on sapphire carried out by Degave et al. [18] indicates that the delay is caused by a Volmer–Weber growth mode governing the first steps of the nucleation process at LT. This type of film deposition leads to the formation of small islands of 5–10 nm in height and about 20 nm in width. Coalescence of the islands occurs after 60 s after which the film thickening continues at its full rate, in this case at $1.04 \mu\text{m h}^{-1}$. Therefore, the last 55 s of growth results theoretically in a 16 nm thick film and an overall thickness of approximately 21–26 nm. This is in very good agreement with the 21 nm film thickness inferred from the reflectivity curve of Fig. 1. A similar delay in LT growth is not observable prior to subsequent LT growth steps as deposition begins on recrystallized GaN. Assuming that a negligible amount of material is lost by desorption during the first recrystallization stage, we can conclude that the thickness of the thin layer of deposit in between the nucleation clusters remains approximately constant throughout the four-cycle process. This can be inferred from Fig. 4 together with the results obtained by calculating the volume of material incorporated in the GaN islands. The conclusion is further supported by the AFM data of Fig. 2, which depicts similar background morphologies for each sample.

In light of the calculations from the AFM data, Fig. 2 clearly indicates that small islands formed during the first recrystallization stage (Fig. 2(a)) very efficiently act as nucleation centers in subsequent recrystallization stages. Nominally about 40 nm of film nucleates on the GaN islands during the second recrystallization stage and only about 60 nm of film is nucleated on the islands during the last two recrystallization stages combined. Therefore one could argue that there is a small decay in the nucleation efficiency as the islands grow in size. This might be caused by the decrease in the effective nucleating area on the high-index planes of the GaN islands as they begin to merge (Fig. 2(c)). The decay is enhanced by the

saturation of growth in the vertical [0001] direction causing material to nucleate only on the high-index surfaces of the islands; a phenomenon similar to the one observed in the standard two-step growth of HT-GaN and in the epitaxial lateral overgrowth (ELOG) technique. The apparent decrease in the amount of LT material nucleated on the islands is most likely accommodated by a small increase in the material loss caused by desorption during the recrystallization stage.

The root mean square (RMS) roughness for the surface of samples A, B and C was 38, 121 and 177 nm, respectively, as obtained from AFM measurements. When the probe wavelength $\lambda \gg \sigma$, where σ designates the RMS roughness, the surface reflectivity at normal incidence can be estimated by [19]

$$R = R_0 \exp \left[- \left(\frac{4\pi\sigma}{\lambda} \right)^2 \right]. \quad (1)$$

In Eq. (1), R_0 signifies the reflectivity of a flat surface with $\sigma = 0$. Using the reflectivity data of Fig. 1, Eq. (1) can be solved for σ . The resulting calculated RMS roughness value for samples A, B and C was 40, 64 and 83 nm, respectively. The theoretical value of the RMS roughness for sample A is in excellent agreement with the measured value as in this case the condition $\lambda \gg \sigma$ is satisfied. Keeping in mind that very little or no material is lost during the recrystallization stages, the large measured RMS roughness for the studied samples is sufficient to explain the decrease in reflectivity between points 2 and 4 (Fig. 1, inset) in the reflectivity data during each recrystallization stage. For samples B and C the condition $\lambda \gg \sigma$ no longer holds and interference effects are not taken into account by Eq. (1). This gives rise to significant discrepancy between the theoretical and experimental results for large RMS roughness values.

The crystalline quality of samples A, B and C was evaluated from the XRD data of Fig. 5. These measurements were carried out in a triple-axis configuration for maximum resolution. The 2θ – Ω rocking curves around the peak of the (0002) symmetrical reflection for hexagonal GaN are shown in the figure. The full-width at half-maximum (FWHM) of these peaks for samples

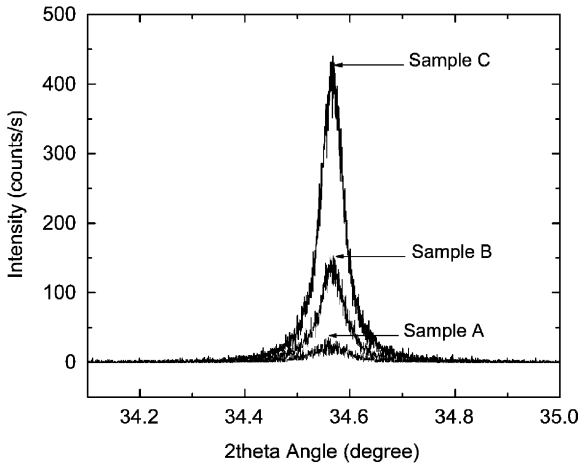


Fig. 5. Comparison of 2θ – Ω XRD rocking curves for each of the studied samples. The narrowing of FWHM for peaks corresponding to the hexagonal (0002) reflection is clearly visible.

A, B and C were 215.3, 202.0 and 186.1 arcsec, respectively. Narrowing of the (0002) diffraction peaks is accompanied by a significant increase in the diffracted intensity as the number of LT-GaN deposition cycles increases and the proportion of the material contained in the islands is increased. These observations suggest that the material, which nucleates on existing GaN islands during the recrystallization step of each cycle, has a smaller density of dislocations with a screw component than the thinner deposit contained in between the islands [9,20]. Additionally, the more pronounced hexagon-shaped plan-view cross-section of the islands in the sample C (Fig. 2(c)) would loosely indicate that the redeposited material is of better crystalline quality in general than the film in between islands; an argument also supported by previous studies indicating that the good quality hexagonal GaN is regrown on the nucleation centers during the recrystallization phase [8]. Further evidence for this statement is provided in the bright field cross-sectional TEM data of Fig. 6 taken from sample C. This is a bright field image and was taken with the substrate tilted about 4° away from the $[2\ 1\ 1\ 0]$ zone normal in the $[0\ 1\ 1\ 0]$ direction. This image indicates a region of higher density of defects, labeled as E, under the island. The defects are well confined

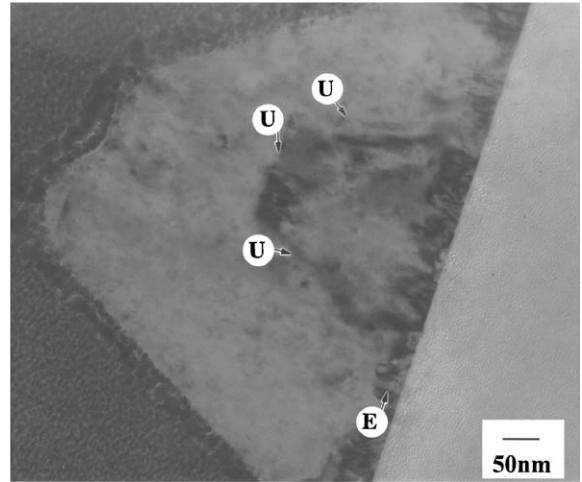


Fig. 6. A bright field cross-sectional TEM image from an individual GaN nucleation island in sample C. The image was taken with the substrate tilted 4° away from the $[2\ 1\ 1\ 0]$ zone normal in the $[0\ 1\ 1\ 0]$ direction. Different regions containing a higher density of defects are labeled in the image. Vertical and horizontal scales are equal in the tilted figure.

within a region close to the sapphire interface. The thickness of this region is roughly the same as the thickness of the thin deposit in between the islands. A region of higher defect content is also contained within the island but is well confined within a boundary labeled as U. The outer regions of the island have less contrasting variations suggesting smaller defect content.

4. Conclusions

A multistep method for the deposition of a GaN nucleation layer was studied. The method consists of alternate low-temperature deposition and annealing steps. Annealing causes the predominantly cubic (111) low-temperature GaN to decompose and recrystallize in nucleation islands. AFM data indicated that the density of the GaN islands remained constant in the consecutive recrystallization steps. The size of the individual islands significantly increased after each annealing step. Observations suggest that these GaN islands efficiently act as nucleation centers for subsequent recrystallization steps. Furthermore, based on film thickness evaluation from AFM, TEM and

reflectivity-data, there was negligible net loss of material from the film surface during the first two NL recrystallization stages. After two cycles of deposition and annealing, GaN redeposition on the (0001) surface was reduced during recrystallization and nucleation mainly took place on the high-index surfaces of each island causing them to grow laterally.

After four cycles, adjacent islands began to coalesce further reducing the allowed surface area for nucleation. This reduction manifested itself as a small decrease in the overall amount of material that was nucleated on the pre-existing GaN islands. As nucleation islands grew in size and the islands started to coalesce the amount of material lost during the recrystallization stage due to desorption slightly increased.

The above observations were supported by in situ reflectometry measurements, which indicated a decrease in the surface reflectivity after consecutive annealing steps due to surface roughening. XRD and TEM measurements also indicated that the material that was redeposited on nucleation islands during each cycle of the multistep process had a smaller defect content than the film contained in between and under the islands. Results indicated that the studied multistep method is an effective way to control the surface morphology of the GaN nucleation layer. This is important in trying to optimize the growth conditions for the subsequent high-temperature overgrowth phase of GaN.

References

- [1] S. Nakamura, T. Mukai, M. Senoh, *Appl. Phys. Lett.* 64 (1994) 1687.
- [2] S. Nakamura, M. Senoh, N. Iwasa, S. Nagahama, *Jpn. J. Appl. Phys.* 34 (1995) L797.
- [3] S. Nakamura, M. Senoh, S. Nagahama, N. Iwasa, T. Yamada, T. Matsushita, H. Kiyoku, Y. Sugimoto, *Jpn. J. Appl. Phys.* 35 (1996) L74.
- [4] S.D. Lester, F.A. Ponce, M.G. Craford, D.A. Steigerwald, *Appl. Phys. Lett.* 66 (1995) 1249.
- [5] S.J. Rosner, E.C. Carr, M.J. Ludowise, G. Girolami, H.I. Erikson, *Appl. Phys. Lett.* 70 (1997) 420.
- [6] S. Nakamura, M. Senoh, S. Nagahama, N. Iwasa, T. Yamada, T. Matsushita, Y. Sugimoto, H. Kiyoku, *Jpn. J. Appl. Phys.* 36 (1997) L1059.
- [7] I. Akasaki, H. Amano, Y. Koide, K. Hiramatsu, N. Sawaki, *J. Crystal Growth* 98 (1989) 209.
- [8] M. Lada, A.G. Cullis, P.J. Parbrook, *J. Crystal Growth* 258 (2003) 89.
- [9] X.H. Wu, P. Fini, E.J. Tarsa, B. Heying, S. Keller, U.K. Mishra, S.P. DenBaars, J.S. Speck, *J. Crystal Growth* 189–190 (1998) 231.
- [10] X.H. Wu, D. Kapolnek, E.J. Tarsa, B. Heying, S. Keller, B.P. Keller, U.K. Mishra, S.P. DenBaars, J.S. Speck, *Appl. Phys. Lett.* 68 (1996) 1371.
- [11] L. Sugiura, K. Itaya, J. Nishio, H. Fujimoto, Y. Kokubun, *J. Appl. Phys.* 82 (1997) 4877.
- [12] J. Chen, S.M. Zhang, B.S. Zhang, J.J. Zhu, G. Feng, X.M. Shen, Y.T. Wang, H. Yang, W.C. Zheng, *J. Crystal Growth* 254 (2003) 348.
- [13] C.R. Lee, S.J. Son, I.H. Lee, J.Y. Leem, S.K. Noh, *J. Crystal Growth* 171 (1997) 27.
- [14] M. Iwaya, T. Takeuchi, S. Yamaguchi, C. Wetzel, H. Amano, I. Akasaki, *Jpn. J. Appl. Phys.* 37 (1998) L316.
- [15] S. Figge, T. Böttcher, S. Einfeldt, D. Hommel, *J. Crystal Growth* 221 (2000) 262.
- [16] D.D. Koleske, A.E. Wickenden, R.L. Henry, J.C. Culbertson, M.E. Twigg, *J. Crystal Growth* 223 (2001) 466.
- [17] D.D. Koleske, A.E. Wickenden, R.L. Henry, W.J. DeSisto, R.J. Gorman, *J. Appl. Phys.* 84 (1998) 1998.
- [18] F. Degave, P. Ruterana, G. Nouet, J.H. Je, C.C. Kim, *Mat. Sci. Eng. B B* 93 (2002) 177.
- [19] H.E. Bennet, J.O. Porteus, *J. Opt. Soc. Am.* 51 (1961) 123.
- [20] B. Heying, X.H. Wu, S. Keller, Y. Li, D. Kapolnek, B.P. Keller, S.P. DenBaars, J.S. Speck, *Appl. Phys. Lett.* 68 (1996) 643.